



Atomic force microscopy imaging of carrageenans from red algae of Gigartinaceae and Tichocarpaceae families

E.V. Sokolova^{a,*}, E.A. Chusovitin^b, A.O. Barabanova^a, S.A. Balagan^{b,c}, N.G. Galkin^{b,c}, I.M. Yermak^a

^a G.B. Elyakov Pacific Institute of Bioorganic Chemistry, Far-East Branch of the Russian Academy of Sciences, Prospect 100-let Vladivostoku, 159, Vladivostok 690022, Russia

^b Institute of Automation and Control Processes of Far Eastern Branch of Russian Academy of Sciences, Radio 5, 690041 Vladivostok, Russia

^c Far Eastern Federal University, 8 Sukhanova Str., 690950 Vladivostok, Russia

ARTICLE INFO

Article history:

Received 31 October 2012

Received in revised form

11 December 2012

Accepted 16 December 2012

Available online 25 December 2012

Keywords:

Carrageenan

Atomic force microscopy

Association

ABSTRACT

In the present article, the atomic force microscopy was applied to investigate macromolecular structures of various carrageenan types including hybrid polysaccharides (κ -, κ/β -, κ/ι -, λ -, and X-carrageenans) depending on polysaccharide concentration. The structures dependence on a polysaccharide concentration also was focused. κ -Carrageenan forms both single and two stranded structures at a low concentration. At high concentrations κ -, κ/β -, and κ/ι -carrageenans form fibrous network-like structures by a side-by-side association type at the same time for κ/ι -carrageenan end-to-end association type also was found. Comparably to κ -carrageenan, κ/β -carrageenan network was more open with coarser fibers while κ/ι -carrageenan structure is characterized with a more flexible network. Honeycombed structures due to end-to-end and side-by-side association types were observed for X-carrageenan, while λ -carrageenan formed honeycombed structures only at high concentrations. In order to investigate topographical parameters of the carrageenans macromolecular structure a new method of the autocorrelation function analysis was used for the first time.

© 2012 Elsevier Ltd. All rights reserved.

1. Introduction

Carrageenan is one of the most important polysaccharides with a wide range of food applications, for instance as a gelling, water holding, stabilizing and thickening agent (Morris, 2007). The importance of carrageenans in pharmaceutical development in last years has been shown. Carrageenans were used to reduce the amount of polymorphic transformation in tabletting (Schmidt, Wartewig, & Picker, 2003), to produce controlled release delivery system (Keppeler, Ellis, & Jacquier, 2009), and to achieve interactions with drugs for modification release systems (Hugerth, 2001). That wide application of these polysaccharides is caused by their physico-chemical properties, which in turn depends on a polysaccharide primary structure. Some carrageenans have been found to exhibit various biological activities, including antitumor (Carlucci, Ciancia, Matulewicz, Cerezo, & Damonte, 1999; Yermak & Khotimchenko, 2003) and anticoagulant activities (Pereira et al., 2005). It is difficult to understand the biological properties of polysaccharides without information on the supramolecular structures because polysaccharides do not function as individual molecules in real systems. From this perspective, the supramolecular structures of polysaccharides

should be investigated to improve their properties understanding on the molecular level (Funami, 2010b).

Carrageenan is the generic name for a family of polysaccharides, obtained by extraction from certain species of red algae (Rhodophyta). They are the mixtures of water-soluble linear sulfated galactans composed basically of an alternating β -(1-3)-D-galactose (G-units) and α -(1-4)-D-galactose (D-units) or α -(1-4)-3,6-anhydro-D-galactose (DA-units) repeating unit (Craigie, 1990). Variation on this basic structure results from the contents of 3,6-anhydrogalactose, location and number of sulfate groups. There are about 20 structures recognized and referred to Greek letters, they are grouped in gelling (κ , ι , β , etc.) and non-gelling (λ , ν , μ , etc.) carrageenans.

Native carrageenans always present complex hybrid structures, and they are generally a mixture of galactans composed of different disaccharide chains (carrabiose), the proportions and structures of which vary with species, ecophysiological and development conditions. The hybrid nature at the molecular level is responsible for the changes in both rheological and conformational properties of the carrageenans compared with those of their homopolymeric types. Earlier with hybrid κ/ι -carrageenan from *Chondrus pinnulatus* (Gigartinaceae) (Yermak et al., 2006), κ/β -carrageenan with hybrid block-like structure (Anastyuk et al., 2011; Barabanova et al., 2005) and X-carrageenan from *Tichocarpus crinitus* (Tichocarpaceae) (Barabanova et al., 2008) and also κ - and λ -carrageenans from *Chondrus armatus* (Yermak, Kim, Titlyanov,

* Corresponding author. Tel.: +7 423 2311430; fax: +7 423 2314050.

E-mail addresses: eka9739@yandex.ru, evsokolova@mail.com (E.V. Sokolova).

Isakov, & Solov'eva, 1999) were isolated from seaweeds harvested at the Russian coast of the Sea of Japan, and their primary structures were described. However, their supramolecular structures have not been investigated yet.

Atomic force microscopy (AFM), a type of scanning probe microscopy, has served as a powerful tool for polysaccharides visualization, not only dispersed or isolated molecules of polysaccharides but also molecular assemblies or supramolecular structures (Funami, 2010b, 2010a). The AFM method allows the supramolecular structure of biopolymers including polysaccharides to be investigated, escaping artifacts obtained as a result of dyeing and fixation accompanying other microscopy techniques. To date, AFM has visualized the supermolecular structures of κ - and ι -carrageenans (Funami et al., 2007; Gunning et al., 1998; Ikeda, Morris, & Nishinari, 2001; MacArtain, Jacquier, & Dawson, 2003; McIntire & Brant, 1999). In the present article, the AFM method was applied to investigate macromolecular structures of various carrageenan types including hybrid polysaccharides. The structures dependence on a polysaccharide concentration also was focused on.

2. Materials and methods

Carrageenan isolation procedure is described elsewhere (Barabanova et al., 2005, 2008; Yermak et al., 1999, 2006). In detail, they were extracted from red algae *T. crinitus*, *C. pinnulatus*, *C. armatus*. Dried algae (10 g) were suspended in distilled water (300 ml) and the polysaccharides were extracted at 90 °C for 3 h in a boiling water bath. The suspensions were centrifuged (2500 × g, 20 min, 20 °C) and the algal residues were re-extracted twice with water for 2 h in a boiling water bath. The supernatants were pooled and concentrated under vacuum to about 100 ml. The polysaccharides were separated into the gelling – KCl-insoluble and non-gelling the KCl-soluble fractions according to Yermak and Khotimchenko (2003). The solutions were exhaustively dialyzed against distilled water, lyophilized, and then used without further treatment. Molecular weights of the used samples were from 200,000 to 500,000 g/mol (Yermak et al., 2012).

The cationic composition was determined by atomic absorption spectroscopy. Sodium and potassium ion contents were determined after mineralization of the carrageenan samples using a microwave digester (MLS-1200 MEGA, Italy) and analyzed by ICP AAS System (Leeman Labs Inc., PS 100, USA) with the following conditions: power – 10 kW, coolant gas – 13 l/min, nebulizer gas pressure – 40 Pa, and pump rate – 1.0 ml/min (Yermak et al., 2012).

The carrageenan samples were dissolved in distilled de-ionized water with mechanical stirring at 50 °C at a concentration of 0.1% (w/v). Then the aqueous test solutions were diluted with distilled de-ionized water at 23 °C to the following final concentration values: 10, 25, 50, and 100 µg/ml. Aliquots (10 µl) of each sample in an aqueous solution were deposited onto freshly cleaved mica, dried at 37 °C for 24 h. Carrageenan morphology was studied by AFM (Solver P47) in tapping contact mode using a 10 nm radius tip in air. During each carrageenan type measurement the AFM tip was not changed. For the first time topographical parameters of the carrageenans macromolecular structure had been calculated by using a new method of the autocorrelation function analysis, which was realized in the program “Calculating of Average Parameters of Objects on Surface” (Author's Certificate No. 2012614467) (Appendix 1).

Of the parameters calculated by means of “Calculating of Average Parameters of Objects on Surface”, we present two of the most interesting with regard to carrageenan: lateral sizes of network cells and normalized volumes (Appendix 2). Lateral sizes of network cells were averaged, since network cells were practically symmetric. A methodological error did not exceed ~1%. With respect to normalized volume was suggested that at the lowest polysaccharide concentration the entire volume of carrageenan evenly spreading on the mica should be visible, we can conclude whether the entire volume of carrageenan is visible at a higher concentration.

3. Results

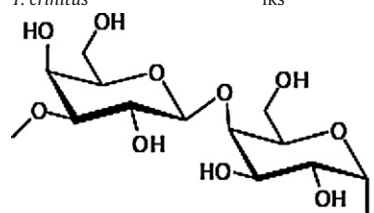
This paper is devoted to the AFM study on a variety of carrageenan types (including hybrids with block-like structure) with a view to relating the primary structure to macromolecular organization observed when the samples are drop deposited onto mica substrates at different bulk concentrations. According to the literature data carrageenans with DA units form three-dimensional networks, which require cross-linking different helices through water molecules or cations (Stortz, 2005). As shown in Table 1 cations contents of the samples is not enough to result in significant gelation process, as their relative values are negligible (e.g. for gelation of 1% solution of κ -carrageenan potassium ions contents should be about 4%).

The following carrageenan structural types were used during the study: κ -, κ/β -, κ/ι -, λ -, and X-types of carrageenans (Table 1). The carrageenan primary structures used were described elsewhere (Barabanova et al., 2005, 2008; Yermak et al., 1999,

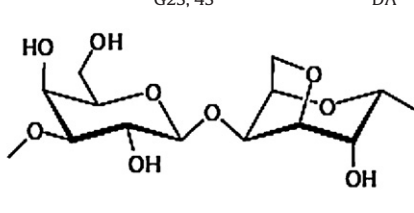
Table 1

The structures of the carrageenans from algae of Gigartineae and Tichocarpaeae families. The letter code nomenclature was used according to Knutsen, Myslabodski, Larsen, and Usov (1994).

Algal species	Carrageenan type	Idealized disaccharide repeat unit		Content per sample dry weight (%)		
		3-Linked	4-Linked	K	Na	Ca
<i>C. armatus</i>	Lambda	G2S	D2S, 6S	0.2	0.5	1.5
<i>C. armatus</i>	Kappa	G4S	DA	0.4	0.6	2.9
<i>C. pinnulatus</i>	Kappa/iota	G4S/G4S	DA/DA2S	0.6	0.8	2.6
<i>T. crinitus</i>	Kappa/beta	G4S/G	DA/DA	0.6	0.5	2.2
<i>T. crinitus</i>	iks	G2S, 4S	DA	0.5	0.7	1.0



G D



G DA

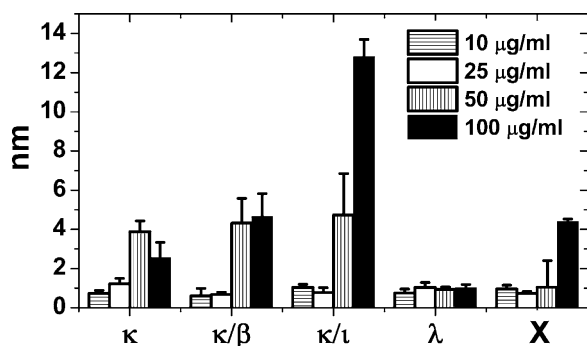


Fig. 1. Average heights of carrageenan structures on the AFM images at various concentrations.

2006). Carrageenans referred to Greek letters differ by number and position of sulfated group and by presence or absence of the 3,6-anhydrogalactose unit (DA).

Fig. 1 illustrates height values at different carrageenan concentrations. According to the diagram (Fig. 1), significant height changes are characteristic only for κ -, κ/β -, and κ/ι -carrageenans and for X-type at 100 $\mu\text{g/ml}$. The height of λ -carrageenan structure imaged with AFM does not undergo any changes during all the concentration range.

Carrageenans with concentrations of 10, 25, 50, and 100 $\mu\text{g/ml}$ were used to be subjected to the AFM observations.

κ -Carrageenan at the lowest concentration value (10 $\mu\text{g/ml}$) (Fig. 2a) forms two types of flexible separated strands that can be visualized on a scale increment (Fig. 2b–d) (gel precursors). Some strands with the height of about 0.4 nm consist of two closely located ones oriented across according to the topography and phase contrast images (Fig. 2b and c). Another type of fibers with the height of about 1 nm is also visualized (Fig. 2d). Branching process is characteristic for both fiber types but with various nature of it.

The increase in a polymer concentration up to 25 $\mu\text{g/ml}$ (Fig. 2e) results in the formation of the network with elongated intertwined fibers forming cells with the average lateral size of 226 nm. The average fiber height is 1.22 ± 0.28 nm suggesting that fibers are likely to be carrageenan double helices. At a high concentration (50 $\mu\text{g/ml}$) κ -carrageenan forms the multilayer netlike structure consisting of some macromolecular associates the height of which reaches up to 3.87 ± 0.79 nm (Fig. 2f). On the AFM image obtained at a concentration of 100 $\mu\text{g/ml}$ one can see at least two κ -carrageenan layers fully cover the mica (substrate) surface (Fig. 2g). Hence, it is difficult to distinguish whether this structure is a superhelical level of association or only a lamination of multihelical aggregates, but the average lateral size of cell compared to the scan at 25 $\mu\text{g/ml}$ increases significantly up to 324 nm.

In the case of hybrid carrageenan, namely κ/β -type, obtained by AFM data differ. When a κ/β -carrageenan concentration of about 10 $\mu\text{g/ml}$ is used, it forms an unordered polymorph structure of gel precursors. Formation of the gel network structure of branching polymer fibers is observed for κ/β -carrageenan under increase a polysaccharide concentration up to 25 $\mu\text{g/ml}$ (Fig. 3a). For high concentration values (Fig. 3b and c) of κ/β -polysaccharide appear to be networks with the cells lateral sizes 242 and 270 nm at 50 and 100 $\mu\text{g/ml}$, respectively. But the fibers, in the case of 100 $\mu\text{g/ml}$, form a multilayer supramolecular structure consisting of more prominent fibers of the network compared to κ -carrageenan (Fig. 3c).

κ/ι -Carrageenan containing a 3,6-anhydrogalactose and three sulfate ester groups per two disaccharide units forms a distinct network structure at a low concentration value of 10 $\mu\text{g/ml}$ average lateral size of which are about 338 nm (Fig. 4a). The fiber heights are about 1.03 ± 0.16 nm suggesting that the fibers are likely to be

carrageenan double helices (Fig. 4a). The increase in a concentration results in the formation of a dense network-like structure, which appears to be a gel network formed in an aqueous film (Fig. 4b).

λ -Carrageenan differs from the rest investigated carrageenan types with a high sulfation degree and the absence of 3,6-anhydrogalactose. The conformation of both the galactose residues of a disaccharide unit corresponds to the ${}^4\text{C}_1$ -chair conformation, and ordered helices are not formed by this structure (Liniers, Helbert, & Van Cutsem, 2005; Piculell, 1995; van de Velde, 2008). All the AFM images of λ -carrageenan demonstrate formation honeycombed structures, a concentration of which per unit of area rises (the lateral size has already reached up to 145 nm at 50 $\mu\text{g/ml}$), while the height of the λ -carrageenan structure image with increasing in an polysaccharide concentration changes insignificantly compared to the other carrageenan types containing DA units (Fig. 5). The height of the λ -carrageenan structure at 50 $\mu\text{g/ml}$ constitutes 1.03 ± 0.26 nm not varying with further the polysaccharide concentration increase (1.01 ± 0.11 nm). This fact is likely to testify the absence of the fiber formation representative for carrageenans with ordered conformations (Fig. 5a and b).

Of the investigated polysaccharides, the primary structure of X-carrageenan built with alternatively linked 1,3-linked β -D-galactopyranosyl-2,4-disulfates and 1,4-linked 3,6-anhydro- α -D-galactopyranosyl residues combines both elements of κ -carrageenan (3,6-anhydrogalactose) and λ -one (a high contents of sulfated groups). X-carrageenan forms honeycombed structures at a low concentration (10 $\mu\text{g/ml}$) similarly to λ -carrageenan. However, average height of the scan (0.95 ± 0.20 nm at 10 $\mu\text{g/ml}$) indicates to the double helical structure formation. The X-carrageenan structure with ordered morphology arises when the concentration reaches up to 50 $\mu\text{g/ml}$ (Fig. 6). In this case, X-carrageenan structure changes to honeycombed structures (1.04 ± 0.13 nm) with large cell-like structures (average sizes is of 309 nm) and complex honeycombed sides (average sizes is of 215 nm) (Fig. 6c). Further increase in the fibers height of X-carrageenan continues with concentration (an image is not included).

As known carrageenans possess water retention properties so it was of interest to estimate the alteration of a carrageenan volume detected on a mica surface and normalized by a concentration (Fig. 7). By means of program "Average Parametres of Objects on Surface" (Author's Certificate No. 2012614467) (Appendix 1) developed at the Institute of Automation and Control Processes of the Far Eastern Branch of the Russian Academy of Sciences "visible volumes" of carrageenans and normalized volumes on the basis of visible volumes were estimated.

The normalized visible volume was estimated for some diverse carrageenan concentrations. A curve of normalized volumes of a concentration values gives some additive information on a polysaccharide supramolecular structure. These indices of κ -, κ/β -, λ -, and X-carrageenans are illustrated in Fig. 7. As shown in the plot, normalized volumes of κ - and κ/β -carrageenans at a concentration of 50 $\mu\text{g/ml}$ increase significantly that appear to be explained with a formation of some cavity in the carrageenans macromolecular structures.

4. Discussion

Height on the AFM images is known to provide information about the degree of molecular associations in quantitative or qualitative (end-to-end and side-by-side types of intermolecular associations for food polysaccharides) manner (Funami, 2010a). The degree of molecular associations, particularly through the side-by-side intermolecular association mode, is partially deducible from the height change information (Funami, 2010a). Hence, at

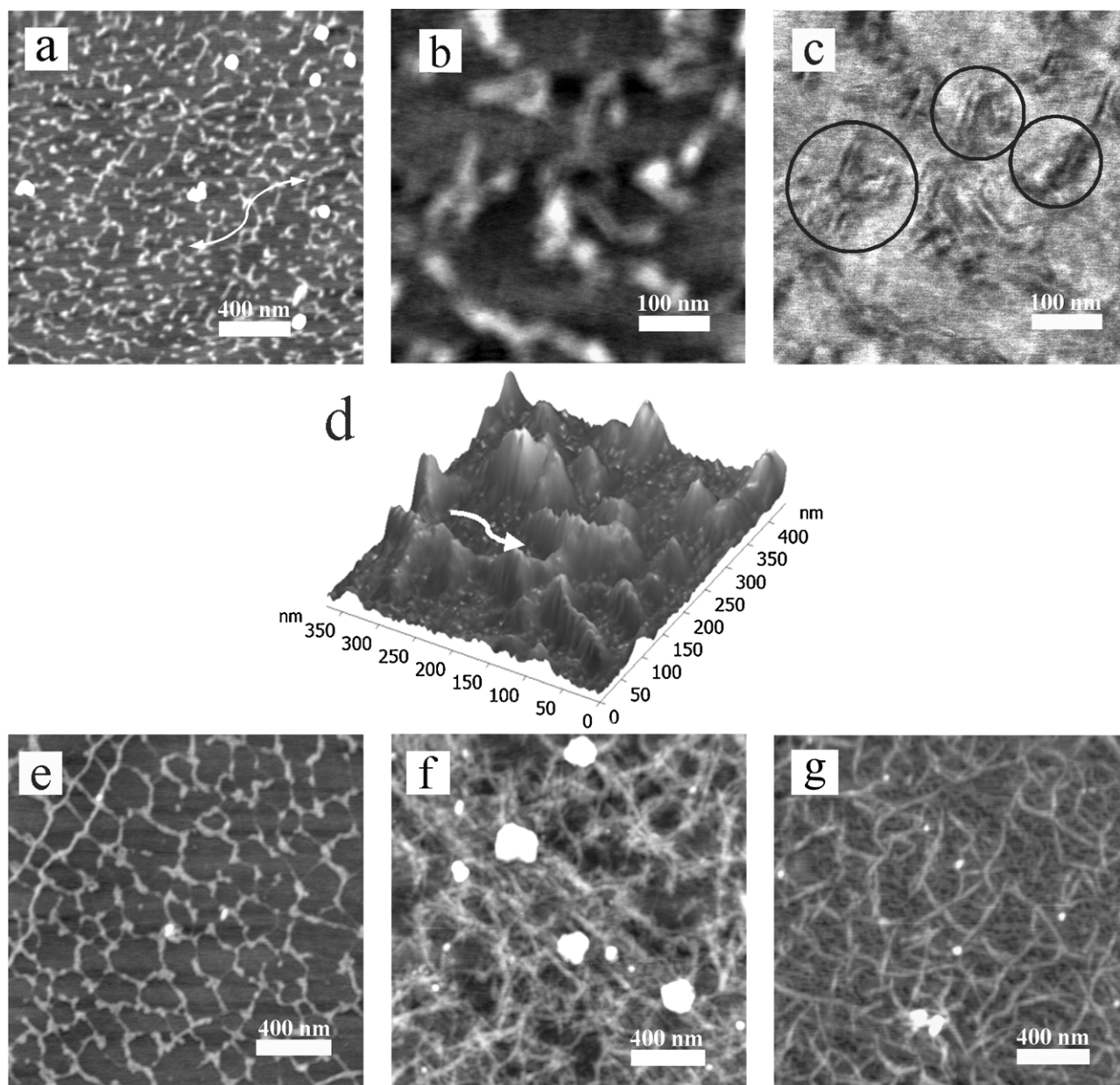


Fig. 2. AFM topography images of κ-carrageenan. (a) 10 μg/ml (arrow points out fibrous branching without a significant height change), (b) 10 μg/ml with an increased scale, (d) κ-carrageenan three dimension image at 10 μg/ml, (e) 25 μg/ml, (f) 50 μg/ml, and (g) 100 μg/ml. AFM phase contrast images of κ-carrageenan: (c) 10 μg/ml with an increased scale.

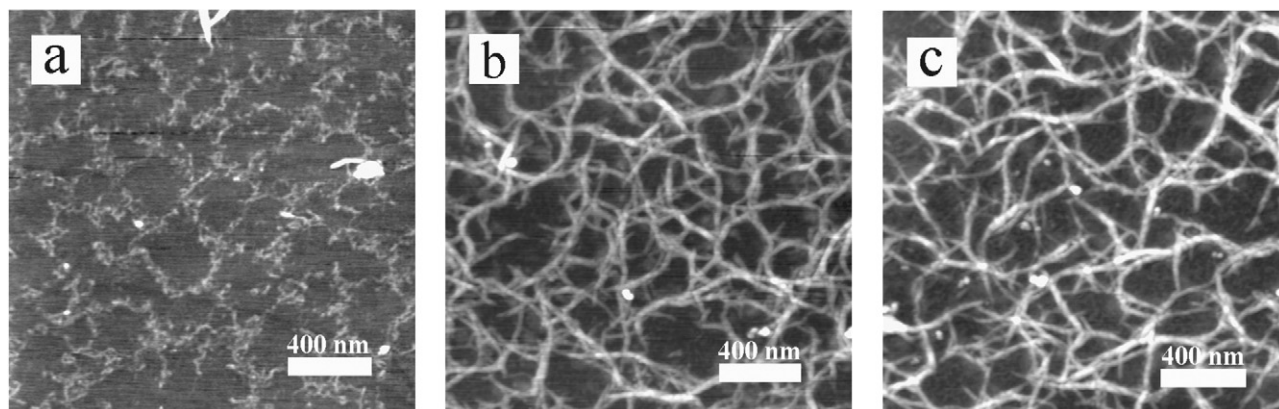


Fig. 3. AFM topography images of κ/β-carrageenan. (a) 25 μg/ml, (b) 50 μg/ml, and (c) 100 μg/ml.

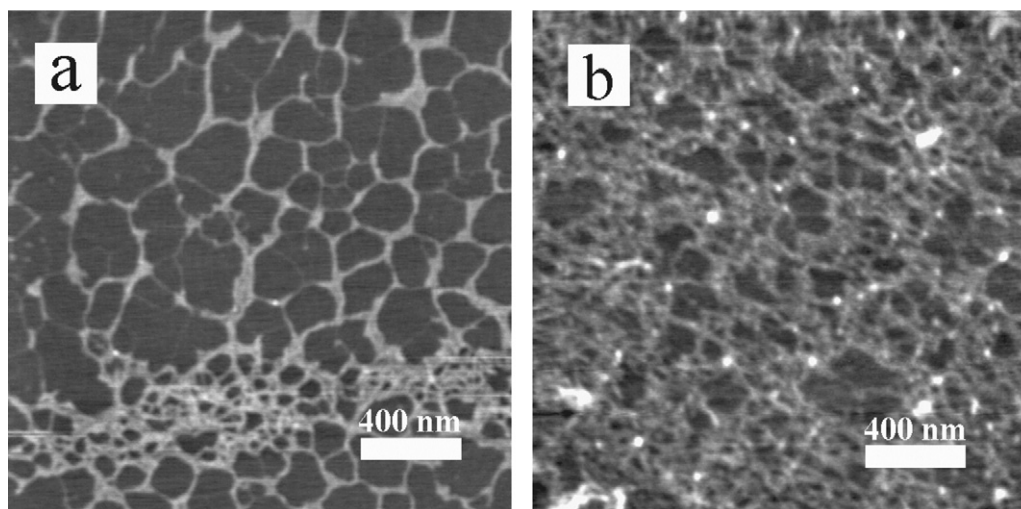


Fig. 4. AFM topography images of κ/ι -carrageenan. (a) 10 $\mu\text{g/ml}$ and (b) 25 $\mu\text{g/ml}$. The arrow points out fiber branching without a significant height change.

the least concentration value (10 $\mu\text{g/ml}$) each type of investigated carrageenans forms structures possessing some unique features. A distinct network structure is represented only by the κ/ι -type while the other carrageenans form incomplete unordered structures. However, κ -carrageenan peculiarities is of especial interest, as the nature of the κ -carrageenan ordered conformation is still a matter of debate, either being a single or double helical state (van de Velde et al., 2005). The current study elucidates that the measured average height of it at 10 $\mu\text{g/ml}$ is of 0.73 ± 0.15 nm, indicating the presence of both single and double stranded helical structures

for this carrageenan type in line with the literature data (Funami et al., 2007; McIntire & Brant, 1999). Existence of single stranded structures confirmed with a height value of some fibers (0.4 nm) arranged parallel as dimmer by side-by-side association (Fig. 2b and c), which hypothetically according to Piculell (1995) issues under association of single helical structures. Those strands result in a branching network formation because of a “side-by-side” interhelical association, which can be seen enough quite on the topography and phase contrast images (Fig. 2b and c). At the same time, the fibers with a height about 1 nm – because of linear polysaccharide double helices formation (Fig. 2d). The formation of single stranded structures by κ -carrageenan visualized with AFM (0.66 ± 0.16 nm) was detected earlier by McIntire and Brant (1999). On the other hand, Funami et al. (2007) observed a scan of κ -carrageenan with double helices (0.84 ± 0.24 nm) in the absence of added salts at the same concentration (10 $\mu\text{g/ml}$). Moreover, branching process of fibers with a height of about 1 nm without increasing in height at the branch points (arrowed in Fig. 2a and c) supports the presence of double helices. The last statement arises from the literature data according to which it considered to be a result of association of polymer polydispersity chains during double helix (Ikeda et al., 2001). The type of branching process when fibers height composes up to double helices is also observed during the current investigation (Fig. 2d). The gel precursors of κ/β -carrageenan (Fig. 3a) appear to be more flexible than those visible for κ -carrageenan. The observed differences are possible to be due to differences in primary structure, as the relative counterions contents for both samples are practically equal (Table 1). At high concentrations κ/β -carrageenan represented as fibrous structures similar to κ -one but with some attributes (Figs. 2 and 3). Its image (Fig. 3b and c) allows formation of a side-by-side interhelical association to be suggested (average height is of 4.65 ± 1.26 nm) at a concentration of 100 $\mu\text{g/ml}$. Distinction of the both carrageenan macromolecular structures, especially at the low concentrations, is possibly because of a hybrid structure of the latter. It is worth noting that furcellaran of the *Furcellaria lumbricalis* red alga with a similar to the κ/β -carrageenan structure forms cell-like structures (Tuvikene et al., 2010). With concentration the lateral sizes of κ - and κ/β -types enhances negligible testifying to the absence of a significant end-to-end association type. It is of interest that κ/β -carrageenan forms coarser strands with a more open network than for κ -type. Analogies changes in supramolecular structure were obtained for κ -carrageenan by the addition of calcium (MacArtain et al., 2003), moreover, those changes in κ -carrageenan network are important to formulate

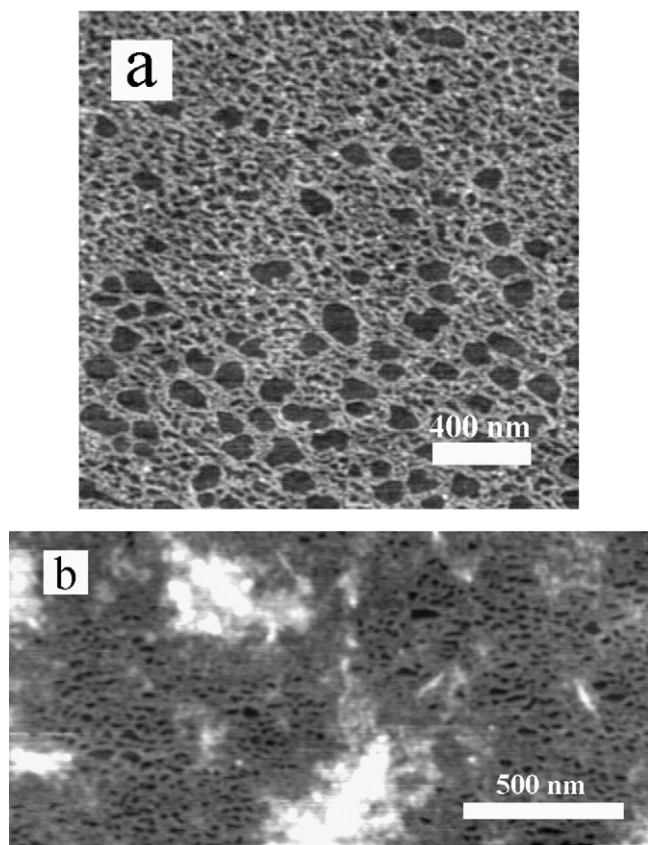


Fig. 5. AFM topography images of λ -carrageenan. (a) 50 $\mu\text{g/ml}$ and (b) 100 $\mu\text{g/ml}$.

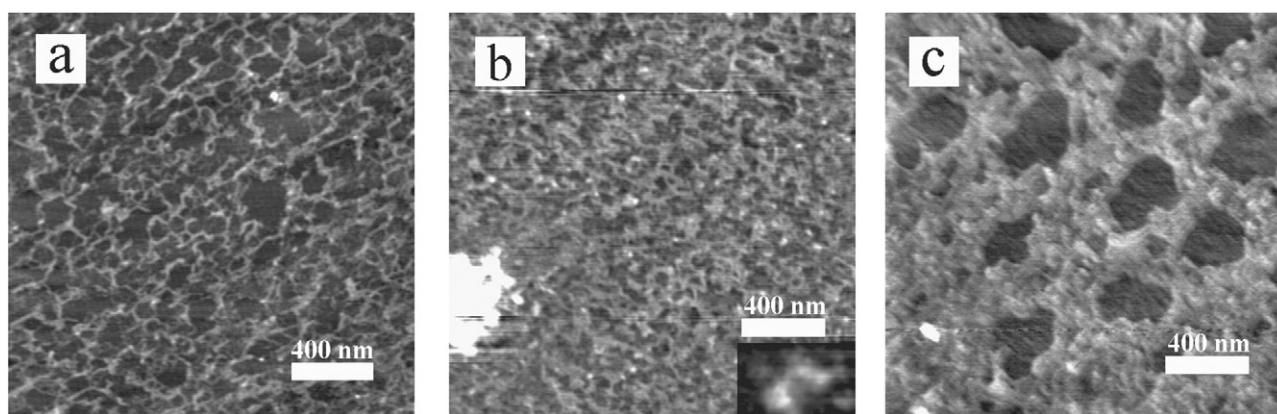


Fig. 6. AFM topography images of X-carrageenan. (a) 10 µg/ml, (b) 25 µg/ml, and (c) 50 µg/ml.

carrageenan beads for drug delivery (Thrimawithana, Young, & Alany, 2011). However, the current study shows that microscopic network corresponds to hybrid κ/β -carrageenan without the addition of any salts. In the case of the κ/ι -carrageenan network at the high concentration is more fine (average lateral sizes increases) due to end-to-end association (Fig. 4b). The network structure appears to be more flexible than for the κ - and κ/β -types networks which could be attributed to the presence of ι repeating units in hybrid κ/ι -carrageenan structure. It is worth noting that according to Ridout, Garza, Brownsey, and Morris (1996) mixed gels of κ - and ι -carrageenans was not detected and independent conformational changes and gelling of separate each product took place. Meanwhile the hybrid κ/ι -carrageenan aggregates quite impressively. According to Funami et al. (2007) AFM imaging has elucidated the difference in the network structures between κ - and ι -carrageenan, and the molecular bundles of ι -carrageenan but κ -type appears to be more flexible with higher homogeneity in the vertical height on the image. The same AFM image as for κ/ι -carrageenan at 10 µg/ml (Fig. 4a) was obtained for pure ι -carrageenan but in the presence of CaCl_2 (Funami et al., 2007). The similar supramolecular structures of κ/ι -carrageenan and ι -type with calcium salt might be explained with the predominant presence of κ -carrageenan units in the hybrid κ/ι -carrageenan sample (Yermak et al., 2006) and/or with negligible amounts of calcium and potassium ions in the carrageenan sample (Table 1). Since a tendency to decrease in a cell size and increase in their relative amount is observed (Fig. 4), so the value of the image mean height (0.76 ± 0.25 nm) must testify to the presence of end-to-end interhelical association preferentially. At high concentrations (50 and 100 µg/ml, AFM images not presented) this carrageenan type forms dense molecular structures,

which could be owing to side-by-side superhelical aggregation. The resolution of AFM images was not enough to their correct interpretation. Insignificant height change of the X-carrageenan fibers (0.95 ± 0.20 nm at 10 µg/ml and 0.73 ± 0.09 nm at 25 µg/ml) testifies of aggregates formation owing to an “end-to-end” association type (Fig. 6b). Hence, supramolecular structure of X-carrageenan at high concentrations forms honeycombed structures by means of end-to-end and side-by-side association types. According to the diagram (Fig. 1), significant height changes are characteristic only for carrageenans containing 3,6-anhydrogalactose. Hence, “side-by-side” association type is proper for carrageenans containing 3,6-anhydrogalactose while “end-to-end” type of interhelical association occurs for X-carrageenan as its height change is less remarkable than for κ , κ/β , and κ/ι . Since λ -carrageenan does not form gel/helices in aqueous solutions, its macromolecular structures at high concentrations differ from the other carrageenans with honeycombed arrangement, fibrous organization is not characteristic for it at all. It should not be overlooked that these structures could also be artifacts formed under high concentration of λ -carrageenan on drying. During air drying, condensation, and displacement of the molecules may occur through so called “molecular combing”, resulting in associations and aggregations forming in situ on mica that are not originally present in test solutions (Funami, 2010a).

Changes of normalized volumes of the polysaccharides containing DA units (Fig. 7) shows presence of some cavities in their macromolecular structures. In the case of κ/β -carrageenan, those cavities are more massive. Further reduction of the normalized volume suggests that the supramolecular structure is formed with a few layers. The normalized volume of λ -carrageenan does not change at the concentration range that could be connected with absence of any cavities in its supramolecular structures. The curve of X-carrageenan normalized volume as its macromolecular structure has an intermediate character (Fig. 7).

5. Conclusion

The AFM method application results in indicating particularities of the primary structure affecting supramolecular structures of these carrageenans. At a low concentration (10 µg/ml) κ/ι -carrageenans is shown to form double helical structures, while κ -carrageenan is characterized both with single and double stranded structures. At high concentrations κ -, κ/β -, and κ/ι -carrageenans form fibrous network-like structures by a side-by-side association type. λ -Carrageenan possessing a random coil conformation in solutions forms honeycombed structures at high concentrations.

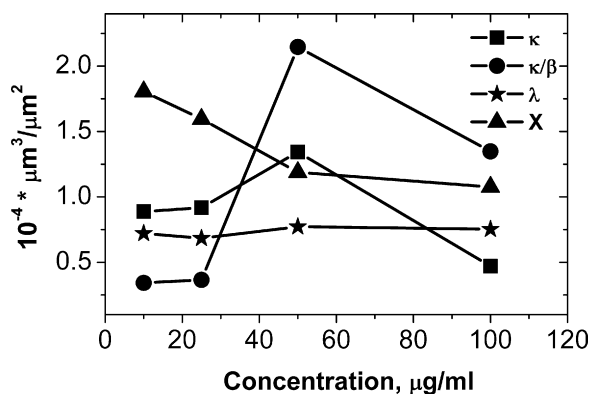


Fig. 7. Normalized volumes. The volume normalized by a concentration of supramolecular structures of κ -, κ/β -, λ -, and X-carrageenans.

Acknowledgements

The study was financially supported by the Russian Academy of Sciences (Program “Molecular and Cellular Biology” of the Presidium of the Russian Academy of Science) and grants of Presidium of the Far Eastern Branch of the Russian Academy of Science.

Appendix 1.

Suggesting that we have an image of some separate objects on a surface, which shape can be well described with a convex polygons, so that we should be able to replace the original image with a mask without significant error in the lateral sizes of the objects.

Autocorrelation function (ACF) is often used for an image analysis and it can be calculated as follows:

$$A(r_p, r_q) = \frac{1}{n_x n_y} \sum_{n=0}^{n_x-1} \sum_{m=0}^{n_y-1} U(x_n, y_m) \cdot U(x_n + r_p, y_m + r_q) \quad (1)$$

where n_x , n_y are the sizes of an image along Ox and Oy axes, respectively, pixels; $U(x_n, y_m)$ are the discrete functions; $x_n = \Delta x \cdot n$; $y_m = \Delta y \cdot m$; $r_p = \Delta x \cdot p$; $r_q = \Delta y \cdot q$; and Δx , Δy are the scanning steps, nm.

Subsequent autocorrelation function evaluation from the mask using Eq. (1) at the central pixel (0; 0) of the ACF and another two pixels with coordinates (0; 1) and (1; 0) relatively to the central point. ACF values for those points will be λ_{00} , λ_{01} , and λ_{10} , respectively. The differences $\lambda_{00} - \lambda_{01}$ and $\lambda_{00} - \lambda_{10}$ represent the sum of the object lengths along Ox (horizontal) and Oy (vertical) axes, respectively. By normalizing the calculated differences to a number of objects, it is possible to determine average sizes of the objects d_x and d_y along Ox and Oy axes, respectively.

$$d_x = \frac{n_x n_y (\lambda_{00} - \lambda_{01})}{n h^2} \quad (2)$$

$$d_y = \frac{n_x n_y (\lambda_{00} - \lambda_{10})}{n h^2} \quad (3)$$

here n is the number of objects; h is the objects height on the mask, nm; n_x , n_y are the size of the mask image along Ox and Oy axes, respectively, pixels.

The total area S occupied by the objects on the surface can be calculated using λ_{00} . By normalizing the calculated area to the object average area one can determine the number of objects.

$$S = \frac{n_x n_y \lambda_{00}}{h^2} \quad (4)$$

$$n = \frac{S}{G} \quad (5)$$

where S is the total area occupied by the objects on the surface, pixels and G is the average area of the objects, pixels.

In Eqs. (2)–(5) we have one free variable. This variable will be determined by the following ratio:

$$\gamma = \frac{G}{d_x d_y}$$

If the object distribution on the surface is uniform, it is possible to make an assumption that γ coefficients calculated for a small part of the image and the whole image should be the same. So using this assumption and the equations set we can obtain the object concentration and average sizes along Ox and Oy axes as well as the object average area and the total area occupied by the object.

Appendix 2.

The term “normalized volume” was used to denote the carrageenan volume (μm^3) per unit of area (μm^2) and normalized by a

factor proportional to the increase in the concentration of the solution – $C_k = C_i/C_0$, where C_i is the concentration of the solution, used to obtain the sample, and C_0 is the minimum concentration which was used for the experiments. Additional normalization on the concentration of the solution makes it easy to analyze the curves of the dependence of the carrageenan normalized volume on the concentration of the solution. Assuming that the density of carrageenan is the characteristic value for specific carrageenan type and does not vary with the concentration one can draw the following conclusions.

1. If the dependence has the form of a line parallel to the horizontal axis, then it is a linear increase in the carrageenan volume. In this case, carrageenan dose not occupy the whole surface – there are some free areas, due to which it is possible to calculate the whole carrageenan volume from an AFM image.
2. If the dependence is decreasing, it means that a continuous layer of carrageenan was formed onto the substrate. There is no free surface, so the volume calculated from the AFM data is less than that actually deposited on the substrate by the amount concentrated in the continuous layer. Carrageenan deposits on the substrate layer-by-layers, and on the AFM image, we observe only the amount of carrageenan concentrated in the incomplete layer, and it is hardly possible to calculate the amount of the completed layer.
3. If the dependence is increasing, it means that the supramolecular structure of carrageenan formed pores which can be filled with liquid.

We use the volume per area unit, rather than a simple volume because application of AFM allows us to calculate only the volume situated in the scanning area, but not the entire carrageenan volume deposited on the substrate surface. Consequently, to be able to compare the carrageenan volume calculated from the AFM images of various sizes, it is necessary to normalize it with the image area. The dimension of the volume per area unit can be written as $\mu\text{m}^3/\mu\text{m}^2$ or μm , if one reduces the fraction. The dimension of μm is interpreted as the carrageenan continuous layer thickness, which will form if carrageenan uniformly distributes over the surface. Summarizing all the above, the normalized volume can be written as:

$$V = \frac{S \cdot \bar{h}}{C_k \cdot S_{im}},$$

where S is the area occupied by carrageenan (μm^2); S_{im} is AFM image area (μm^2); and \bar{h} is the average height of the supramolecular structure of the carrageenan (μm). The value \bar{h} is determined from the histogram of the AFM images point height distribution. As mica surface is atomically smooth, and at moderate concentrations of the carrageenan (to 25 $\mu\text{g}/\text{ml}$) it occupies a small part of the AFM image, the histogram will be a superposition of two peaks: one corresponding to the substrate, and another – to carrageenan. By decomposition of the histogram into two peaks (e.g. using a software package Origin 9.0), one can obtain the position of the peak maxima, and the difference between them will give us the required average height of the supramolecular carrageenan structure. The area occupied with carrageenan was calculated using the program “Calculating of Average Parameters of Objects on Surface”, which algorithm is described in Appendix 1.

References

- Anastyuk, S. D., Barabanova, A. O., Correc, G., Nazarenko, E. L., Davydova, V. N., Helbert, W., et al. (2011). Analysis of structural heterogeneity of κ/β -carrageenan oligosaccharides from *Tichocarpus crinitus* by negative-ion ESI and tandem MALDI mass spectrometry. *Carbohydrate Polymers*, 86, 546–554.

- Barabanova, A. O., Shashkov, A. S., Glazunov, V. P., Isakov, V. V., Nebylovskaya, T. B., Helbert, W., et al. (2008). Structure and properties of carrageenan-like polysaccharide from the red alga *Tichocarpus crinitus* (Gmel.) Rupr. (Rhodophyta, Tichocarpaceae). *Journal of Applied Phycology*, 20, 1013–1020.
- Barabanova, A. O., Yermak, I. M., Glazunov, V. P., Isakov, V. V., Titlyanov, E. A., & Solov'eva, T. F. (2005). Comparative study of carrageenans from reproductive and sterile forms of *Tichocarpus crinitus* (Gmel.) Rupr. (Rhodophyta, Tichocarpaceae). *Biochemistry (Moscow)*, 70, 430–437.
- Carlucci, M. J., Ciancia, M., Matulewicz, M. C., Cerezo, A. S., & Damonte, E. B. (1999). Antiherpetic activity and mode of action of natural carrageenans of diverse structural types. *Antiviral Research*, 43, 93–100.
- Craigie, J. S. (1990). Cell wall. In K. M. Cole, & G. Sheath (Eds.), *Biology of the red algae* (pp. 221–257). Cambridge: Cambridge University Press.
- Funami, T. (2010a). Atomic force microscopy imaging of food polysaccharides. *Food Science Technology Research*, 16, 1–12.
- Funami, T. (2010b). Atomic force microscopy imaging of food polysaccharides in relation to rheological properties. *Food Science and Technology Research*, 16, 13–22.
- Funami, T., Hiroe, M., Noda, S., Asai, I., Ikeda, S., & Nishinari, K. (2007). Influence of molecular structure imaged with atomic force microscopy on the rheological behavior of carrageenan aqueous system in the presence or absence of cations. *Food Hydrocolloids*, 21, 617–629.
- Gunning, A. P., Cairns, P., Kirby, A. R., Round, A. N., Bixler, H. J., & Morris, V. J. (1998). Characterising semi-refined iota-carrageenan networks by atomic force microscopy. *Carbohydrate Polymers*, 36, 67–72.
- Hugerth, A. M. (2001). Micropolarity and microviscosity of amitriptyline and dextran/sulfate carrageenan–amitriptyline systems: The nature of polyelectrolyte–drug complexes. *Journal of Pharmacology Sciences*, 90, 1665–1670.
- Ikeda, S., Morris, V. J., & Nishinari, K. (2001). Microstructure of aggregated and nonaggregated kappa-carrageenan helices visualized by atomic force microscopy. *Biomacromolecules*, 2, 1331–1337.
- Keppeler, S., Ellis, A., & Jacquier, J. C. (2009). Cross-linked carrageenan beads for controlled release delivery systems. *Carbohydrate Polymers*, 78, 937–940.
- Knutsen, S. H., Myslabodski, D. E., Larsen, B., & Usov, A. I. (1994). A modified system of nomenclature for red algal galactans. *Botanica Marina*, 37, 163–169.
- Liners, F., Helbert, W., & Van Cutsem, P. (2005). Production and characterization of a phage-display recombinant antibody against carrageenans: Evidence for the recognition of a secondary structure of carrageenan chains present in red algae tissues. *Glycobiology*, 15, 849–860.
- MacArtain, P., Jacquier, J. C., & Dawson, K. A. (2003). Physical characteristics of calcium induced kappa-carrageenan networks. *Carbohydrate Polymers*, 53, 395–400.
- McIntire, T. M., & Brant, D. A. (1999). Imaging of carrageenan macrocycles and amylose using noncontact atomic force microscopy. *International Journal of Biological Macromolecules*, 26, 303–310.
- Morris, V. J. (2007). Gels. In P. Belton (Ed.), *The chemical physics of food* (pp. 365–397). Oxford, UK: Blackwell Science Ltd.
- Pereira, M. G., Benevides, N. M. B., Melo, M. R. S., Valente, A. P., Melo, F. R., & Mourao, P. A. S. (2005). Structure and anticoagulant activity of sulfated galactan from the red alga, *Gelidium crinale*. Is there a specific structural requirement for the anticoagulant action. *Carbohydrate Research*, 340, 2015–2020.
- Piculell, L. (1995). Gelling carrageenans. In A. M. Stephen (Ed.), *Food polysaccharides and their applications* (pp. 205–244). New York: Marcel Dekker Inc.
- Ridout, M. J., Garza, S., Brownsey, G. J., & Morris, V. J. (1996). Mixed iota–kappa carrageenan gels. *International Journal of Biological Macromolecules*, 18, 5–8.
- Schmidt, A. G., Wartewig, S., & Picker, K. M. (2003). Potential of carrageenans to protect drugs from polymorphic transformation. *European Journal of Pharmaceutics and Biopharmaceutics*, 56, 101–110.
- Stortz, C. A. (2005). Carrageenans: Structural and conformational studies. In K. J. Yarema (Ed.), *Handbook of carbohydrate engineering* (pp. 211–245). Boca Raton, USA: Taylor and Francis.
- Thrimawithana, T. R., Young, S., & Alany, R. G. (2011). Effect of cations on the microstructure and in-vitro drug release of kappa- and lambda-carrageenan liquid and semi-solid aqueous dispersions. *Journal of Pharmacy and Pharmacology*, 63, 11–18.
- Tuvikene, R., Truus, K., Robal, M., Volobujeva, O., Mellikov, E., Pehk, T., et al. (2010). The extraction, structure, and gelling properties of hybrid galactan from the red alga *Furcellaria lumbricalis* (Baltic Sea, Estonia). *Journal of Applied Phycology*, 22, 51–63.
- van de Velde, F. (2008). Structure and function of hybrid carrageenans. *Food Hydrocolloids*, 22, 727–734.
- van de Velde, F., Antipova, A. S., Rollema, H. S., Burova, T. V., Grinberg, N. V., Pereira, L., et al. (2005). The structure of j/i-hybrid carrageenans: II. Coil–helix transition as a function of chain composition. *Carbohydrate Research*, 340, 1113–1129.
- Yermak, I. M., Barabanova, A. O., Aminin, D. L., Davydova, V. N., Sokolova, E. V., Kim, Y. H., et al. (2012). Effects of structural peculiarities of carrageenans on their immunomodulatory and anticoagulant activities. *Carbohydrate Polymers*, 87, 713–720.
- Yermak, I. M., Barabanova, A. O., Glazunov, V. P., Isakov, V. V., Kim, Y. H., Shin, K. S., et al. (2006). Carrageenan from cystocarpic and sterile plants of *Chondrus pinnulatus* (Gigartinales, Rhodophyta) collected from the Russian Pacific coast. *Journal of Applied Phycology*, 18, 361–368.
- Yermak, I. M., & Khotimchenko Yu, S. (2003). Chemical properties, biological activities and applications of carrageenan from red algae. In M. Fingerman, & R. Nagabhushanam (Eds.), *Recent advances in marine biotechnology* (pp. 207–210). USA/UK: Science Publishers Inc.
- Yermak, I. M., Kim, Y. H., Titlyanov, E. A., Isakov, V. V., & Solov'eva, T. F. (1999). Chemical structure and gel properties of carrageenan from algae belonging to the Gigartinales and Tichocarpaceae, collected from the Russian Pacific coast. *Journal of Applied Phycology*, 11, 41–48.